

Role of Particle Size on Flotation Kinetics of Turkish Sphalerite Ores

OKTAY BAYAT*, METIN UCURUM† and COLIN POOLE‡

Cukurova University, Mining Engineering Department, Balçalı, 01330 Adana, Turkey

Tel.: +90-322-3386119; fax: +90-322-3386126

E-mail: obayat@cukurova.edu.tr

The effects of size distribution on the flotation behaviour of sphalerite have been investigated in terms of kinetic parameters. In experimental studies, sub-samples of a Turkish sphalerite ore were ground for different times using a laboratory ball mill. Timed batch tests were then undertaken using a pilot flotation column and the resulting recovery/time data were used in kinetic modelling. Results indicated that sphalerite floated rapidly at a medium particle size distribution ($d_{80} = 0.125$ mm in this case). In addition, a statistical analysis of data demonstrated that the flotation rate constant corresponded to a first-order model with rectangular distribution of floatabilities given by the equation

$$r = R_{\infty} \left\{ 1 - \frac{1}{k_2 t} [1 - \exp(-k_2 t)] \right\}.$$

Key Words: Sulphide ores, Column flotation, Flotation kinetics, Mineral processing.

INTRODUCTION

At present, over two billion tons of various ores and coal are treated annually by flotation processes¹. Kinetic models are often used to analyze batch flotation data and to evaluate the effects of various parameters such as flotation reagent dosages and equipment operating conditions². Therefore, numerous researchers have studied the kinetic aspects of froth flotation, paying special attention to the size of particles, bubbles and their complex interactions^{3–5}. Particle liberation plays an important role in flotation processes, as demonstrated by studies on the detachment of particles during bubble coalescence, or by comparison of kinetic parameters for liberated or locked particles. The size to which ore to be processed should be ground in order to optimize processing profitability while taking into account that metallurgical balance and size-reduction cost is a very important parameter⁶. Mathematical flotation models which incorporate both a recovery and a rate function can completely describe flotation time-recovery profiles⁷. In an

†Cukurova University, Vocational College of Karaisali, Mining Department, Adana, Turkey; E-mail: cevher@cukurova.edu.tr

‡Leeds University, Department of Mining & Mineral Engineering, Leeds, LS2 9JT, UK; E-mail; c.poole@leeds.ac.uk

early flotation model of the 1930's, as reviewed by Dowling *et al.*⁸, recovery was expressed as an exponential function of time. Subsequently, many flotation models have been proposed and published in the literature. Lynch *et al.*⁹ have conveniently defined three categories for these models: (i) empirical models (ii) probability models and (iii) kinetic models. Empirical models are too specific to their environment and usually involve a trial and error feedback approach to optimization, while probability models can reduce to kinetic models in certain constraints. Several kinetic flotation models have been evaluated by Dowling *et al.*⁸ using data from batch-scale flotation of a simple porphyry copper ore. Some of these are summarized and commented upon in Table-1.

TABLE-1
DESCRIPTION OF SOME KINETIC FLOTATION MODELS

No.	Model	Formula	Remarks
1	Classical first-order model	$r = R_{\infty} [1 - \exp(-k_1t)]$	Model appears to predict values best when recovery is especially low
2	First-order model with rectangular distribution of floatabilities	$r = R_{\infty} \left\{ 1 - \frac{1}{k_2t} [1 - \exp(-k_2t)] \right\}$	Rectangular distribution of floatabilities gives an added flexibility and, therefore, should be a better form of the first-order process. Fit to data is reported to be the best of all models tested, and confidence limits for the parameters k_2 and R_{∞} are very narrow.
3	Second-order kinetic model	$r = \frac{R_{\infty}^2 k_3 t}{1 + R_{\infty} k_3 t}$	Two parameter expression describing the flotation of a mono-disperse feed with particles having a constant floatability.
4	Second-order model with rectangular distribution of floatabilities	$r = R_{\infty} \left\{ 1 - \frac{1}{k_4 t} [\ln(1 + k_4 t)] \right\}$	The assumed two-order form introduces additional parameter dilution in the confidence intervals. The fit to the observed data and the confidence intervals decreases as fractional recovery approaches 1.0.

Note: r = fractional recovery at time t , R_{∞} = fractional ultimate recovery, k_n = rate constants ($n = 1,2,3,4$)

In this study, the four kinetic flotation models described in Table-1 were tested on batch flotation time-recovery profiles for size distributions of a Turkish sphalerite ore using a pilot plant flotation column. Understanding and interpreting changes in the values of R_{∞} and k are very important and can often be misleading². For instance, changing one condition in a laboratory operation (*e.g.*, gas flow rate) may lead to a significant change in the value of k but not R_{∞} . Thus, it is concluded that the gas rate has a significant effect on the rate at which mass is being removed from the flotation cell, without influencing the ultimate amount

removed. Likewise, changing the collector dosage, for instance, may lead to a significant change in the value of R_{∞} but not k . This shows that the overall proportion which can be ultimately floated has changed, without any impact on the flotation time required. However, in many laboratory flotation studies, changing one condition leads to a change in both R_{∞} and k values under different conditions. For instance, changing one condition may lead to an increase in k but a decrease in R_{∞} , while selectivity between the valuable and gangue minerals might be unchanged, increased or decreased depending only on the combined measure of k and R_{∞} values. One method of overcoming the difficulty of comparing k and R_{∞} values is to introduce a modified rate constant which takes into account both ultimate recovery and rate constant. Consequently, a selectivity index based on this modified rate constant between different minerals in a flotation system can be obtained. The selectivity index (or relative rate constant) of mineral I (Zn in this case) over mineral II (Fe in this case) in a flotation system is defined as the ratio of the modified rate constant of mineral I to that of mineral II:

$$SI(I/II) = \frac{K_m \text{ of mineral (I)}}{K_m \text{ of mineral (II)}} \quad \dots (1)$$

The relative rate constant is the measure of flotation separation selectivity of mineral I over mineral II. The least squares method is used to obtain the best fit of the models to the experimental data by minimizing the sum of squares. In the present study, eight increments (data points: 0.5, 1, 2, 3, 5, 10, 20 and 30 min of flotation time) were obtained for each batch test and then used to determine the flotation rate of sphalerite and the selectivity index (or relative rate constant) in order to set the basis for particle liberation.

EXPERIMENTAL

Experiments were carried out using samples of sphalerite ore supplied by Postalli Mining Company, Kayseri, Turkey. The chemical composition of the sample is shown in Table-2. A mineralogical analysis was conducted on polished hand samples; a typical section is shown in Fig. 1. Major ore minerals identified were galena, sphalerite and pyrite as the primary sulphides, with smithsonite, cerussite, anglesite and goethite as the secondary oxide-hydroxide-carbonate minerals. Collecting agents (Aerofloat 7048 and Aerofloat 7279) used in the study were supplied by Cytec International, Holland. Sodium silicate and copper sulphate were obtained from Sigma Chemicals and Fluka Chemicals, respectively. Tap water was used throughout the experiments. The pulp pH was adjusted using lime.

In a typical flotation test, a representative 0.5 kg sub-sample was ground in a 200 mm diameter x 200 mm stainless steel mill at a pulp density of 70% by weight using a charge of 5 kg of stainless steel balls. The grinding times were 5, 10, 15 and 20 min, giving particle size distributions of $d_{80} = 0.180, 0.125, 0.075$ and 0.063 mm, respectively. Individual tests were performed in a flotation column shown schematically in Fig. 2. The column was constructed in stainless steel, 135

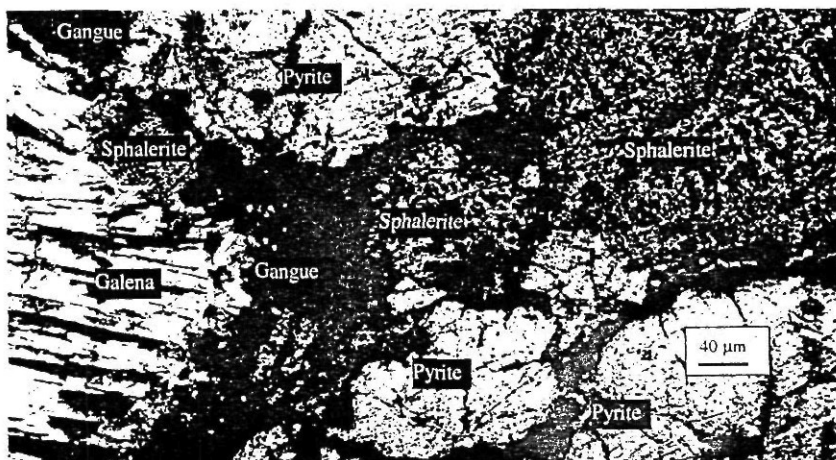


Fig.1 Micrograph of sphalerite ore (using an Olympus BH2-UMA microscope)

mm in diameter and 2800 mm in total length. The downcomer was 45 mm in diameter and 1000 mm in length. The gas entry point was located in the column, bottom section pointing upwards and the slurry was introduced into the downcomer *via* a nozzle to form a jet, compared to the conventional column where the feed is introduced near the froth/slurry interface. Feed was introduced into the feed sump and a fixed speed feed pump fed the material into the aerator where slurry was injected into the feed downcomer. Air was drawn in from atmosphere at an uncontrolled rate *via* an air inlet. The induced bubbles with floatable

TABLE-2
CHEMICAL COMPOSITION OF SPHALERITE SAMPLE

Species	(Wt%)
SiO ₂	22.52
CaO	1.70
MgO	8.82
Pb	0.87
Zn	16.47
Fe	23.72
Cu	0.29
Cd	0.09
Mn	0.04
Au	Trace
Ag	0.007
L.O.I.	22.60
Others	25.47

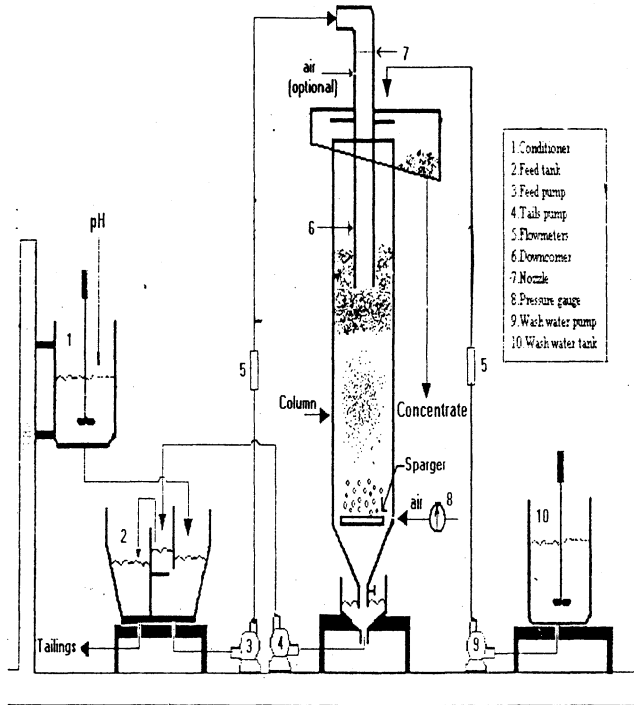


Fig. 2 Schematic of the experimental flotation column

particles attached to them rose to the top to be discharged as concentrate (which was usually washed), whilst the remainder of the feed slurry containing floatable and non-floatable material settled to the base of the column. The base was equipped with a secondary bubble injection system *via* a sparger which introduced small air bubbles. Here, the floatable material had a second opportunity for bubble attachment, thus simulating two flotation units in series. The non-floatable material discharged *via* the column base as tailings at a controlled rate. Instead of the tailings discharging directly to the tailings sump, it was fed to a dummy sump inside the feed sump. The dummy sump was designed with two outlets, a high level-overflow which fed the tails sump and a non-return orifice connecting with the feed sump. Fluctuations in the feed to the flotation column were eliminated, as a constant volumetric flowrate was pumped to the flotation column through a fixed speed pump. As the level of the feed sump dropped, more tailings slurry flowed from the dummy sump to the feed sump, owing to larger level differences, and *vice versa*. The excess tailings overflowed to the actual tails sump. After each test, products were vacuum filtered, dried in an oven at $90 \pm 5^\circ\text{C}$ to constant weight and assayed for Zn and Fe using an atomic absorption spectrophotometer. Design and test parameters are presented in Table-3.

TABLE-3
FLOTATION COLUMN DESIGN AND OPERATING SPECIFICATIONS

Column variable	Pilot column
Diameter (mm)	135
Total height (mm)	3200
Downcomer diameter (mm)	45
Downcomer height (mm)	1000
Froth height	Variable
Wash water rate	Not applied
Feed per cent solids (%)	7.5
d_{80} (mm)	0.063, 0.075, 0.125 and 0.180
Superficial feed velocity (mm/s)	22
Superficial air velocity (mm/s)	13
Sparger type	Internal
pH	12 (with lime)
Na_2SiO_3 (g/t)	250
CuSO_4 (g/t)	575
Aero 7048 + Aero 7279 (g/t)	700

RESULTS AND DISCUSSION

Four separate size distributions were used to investigate the effects of particle size on froth structures, *i.e.*, $d_{80} = 0.063, 0.075, 0.125$ and 0.180 mm. The size analyses of the feed and four individual fractions are shown in Fig. 3. A single data set of Zn flotation recoveries for each particle size distribution was chosen

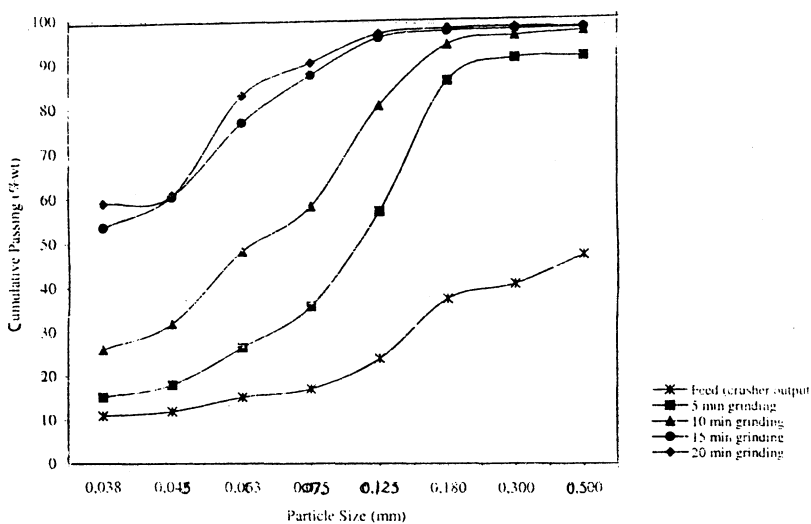


Fig. 3 Particle size distribution of sphalerite sample after different grinding times

to evaluate the models outlined in Table-1. The parameters in each model were calculated from the test data using non-linear regression. To determine kinetic parameters such as flotation rate constant (k) and the ultimate recovery (R_{∞}), a statistical programme SPSS for Windows 9.0 was used to treat the data in the mode "non-linear regression".

Parameters from each model for different particle size distributions are presented in Tables 4-7. All kinetic models tested gave a similar fit to the

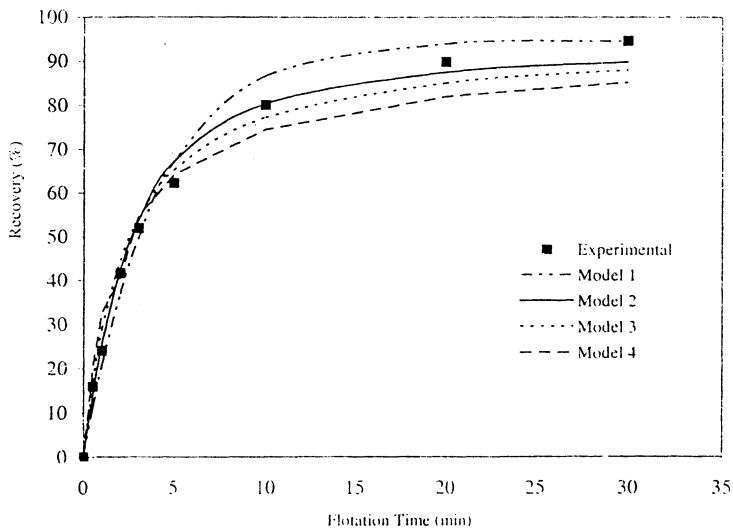


Fig. 4 Comparison of kinetic models fitted to data set for 0.180 mm particle size

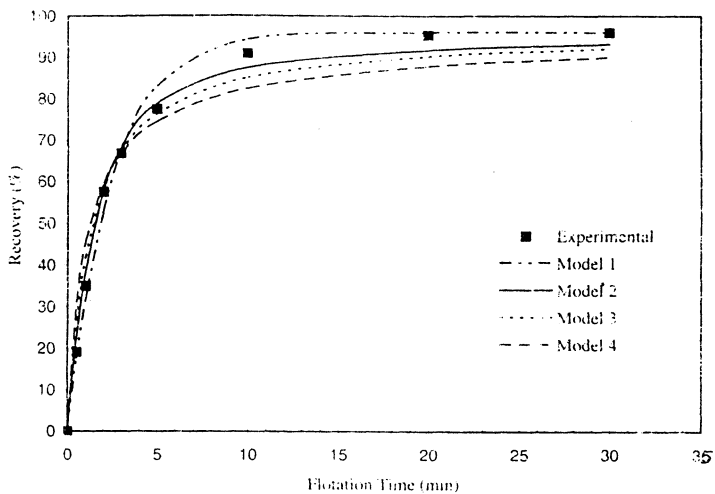


Fig. 5 Comparison of kinetic models fitted to data set for 0.125 mm particle size

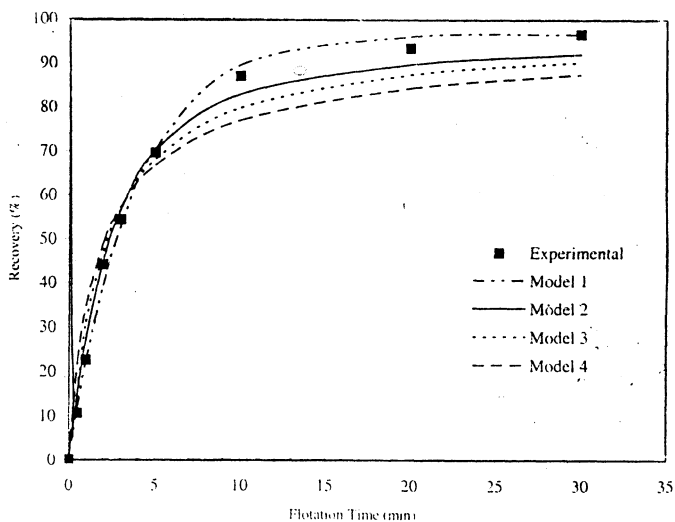


Fig. 6 Comparison of kinetic models fitted to data set for 0.075 mm particle size

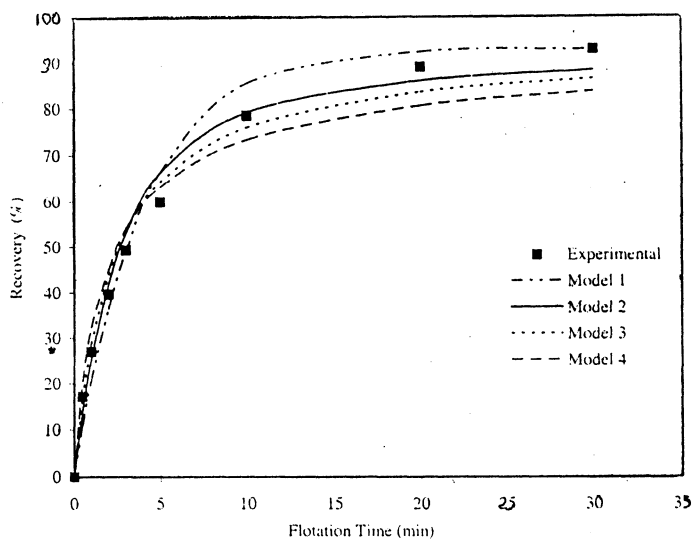


Fig. 7 Comparison of kinetic models fitted to data set for 0.063 mm particle size

experimental data, but model 2 demonstrated an excellent fit for the particle sizes studied. When comparing the fitting curves in Fig. 4–7, it was observed that only very small differences occurred amongst the tested models at the beginning of flotation (up to 5 min. flotation time). However, after this period model 2 was considered to be the best fit and the most suitable for understanding the Zn flotation process. Similar findings were also observed for a simple porphyry copper ore and a complex sulphide ore^{8,10}. The reason for this, also indicated by Xu *et al.*¹⁰, appears to be that model 2 is simple and mathematically stable;

therefore, it can be used in a wide range of k_2 and R_∞ values. Calculated selectivity index values are presented in Table-8. The Zn/Fe selectivity index values at the finer sizes (*i.e.*, $d_{80} = 0.075$ mm and 0.063 mm) were slightly higher than those at $d_{80} = 0.180$ mm when considering model 2 as the best fit for Zn flotation. However, overall analysis of the flotation rate constant and selectivity index data indicated that $d_{80} = 0.125$ mm was the optimum particle size for Zn flotation.

TABLE-4
PARAMETERS OBTAINED FROM MODEL 1 FIT TO DATA SET FOR Zn AND Fe

	$d_{80} = 0.180$ mm		$d_{80} = 0.125$ mm		$d_{80} = 0.075$ mm		$d_{80} = 0.063$ mm	
	Zn	Fe	Zn	Fe	Zn	Fe	Zn	Fe
R_∞	0.9453	0.2748	0.9303	0.3181	0.9660	0.2869	0.9297	0.2089
k_1	0.2470	0.1045	0.4005	0.0788	0.2607	0.0990	0.2495	0.0920
K_m	0.2334	0.0287	0.3846	0.0251	0.2518	0.0284	0.2320	0.0192
R^2	0.9912	0.9860	0.9942	0.9649	0.9966	0.9954	0.9884	0.9706

TABLE-5
PARAMETERS OBTAINED FROM MODEL 2 FIT TO DATA SET FOR Zn AND Fe

	$d_{80} = 0.180$ mm		$d_{80} = 0.125$ mm		$d_{80} = 0.075$ mm		$d_{80} = 0.063$ mm	
	Zn	Fe	Zn	Fe	Zn	Fe	Zn	Fe
R_∞	0.8984	0.2510	0.9318	0.2908	0.9260	0.2619	0.8839	0.1907
k_2	0.6642	0.2640	1.1230	0.1934	0.7035	0.2490	0.6710	0.2300
K_m	0.5967	0.0663	1.0464	0.0562	0.6476	0.0652	0.5931	0.0438
R^2	0.9936	0.9700	0.9964	0.9460	0.9960	0.9826	0.9880	0.9508

TABLE-6
PARAMETERS OBTAINED FROM MODEL 3 FIT TO DATA SET FOR Zn AND Fe

	$d_{80} = 0.180$ mm		$d_{80} = 0.125$ mm		$d_{80} = 0.075$ mm		$d_{80} = 0.063$ mm	
	Zn	Fe	Zn	Fe	Zn	Fe	Zn	Fe
R_∞	0.8799	0.2394	0.9209	0.2754	0.9028	0.2498	0.8656	0.1813
k_3	0.0047	0.0058	0.0081	0.0035	0.0049	0.0052	0.0048	0.0065
K_m	0.0040	0.0014	0.0075	0.0009	0.0044	0.0013	0.0042	0.0012
R^2	0.9916	0.9620	0.9896	0.9359	0.9884	0.9724	0.9880	0.9416

When grinding data from the actual Kayseri plant were analyzed, it was observed that the d_{80} size of the flotation feed (taken from the overflow of the spiral classifier) was 0.2 mm, suggesting a lower flotation rate constant and inefficient separation of sphalerite from pyrite. Fine particles typically show slow recovery rates, owing to decreased particle-bubble collisions, and are prone to entrainment. Moreover, very small particles tend to have large specific areas, which can lead to excessive adsorption of reagents and other effects associated

with chemically active particles¹¹. The destruction of froth by hydrophobic particles is size-dependent, and there seems to be an optimum size range for particles to stabilize or destabilize the froth. In the laboratory column tests with fine size fractions (*i.e.*, $d_{80} = 0.063$ mm), froth stability was observed to be higher and froth volume was larger, whereas with coarse size fractions (*i.e.*, $d_{80} = 0.180$ mm), the froth was unstable and the froth volume was lower. Therefore, a medium size particle fraction ($d_{80} = 0.125$ mm in this case) was judged to result in a better overall flotation performance, confirming the modelling exercise.

TABLE-7
PARAMETERS OBTAINED FROM MODEL 4 FIT TO DATA SET FOR Zn AND Fe

	$d_{80} = 0.180$ mm		$d_{80} = 0.125$ mm		$d_{80} = 0.075$ mm		$d_{80} = 0.063$ mm	
	Zn	Fe	Zn	Fe	Zn	Fe	Zn	Fe
R_{∞}	0.8517	0.2282	0.9000	0.2613	0.8747	0.2378	0.8383	0.1724
k_4	1.2100	0.4250	2.2420	0.3000	1.2950	0.4000	1.2260	0.3640
K_m	1.0350	0.0969	2.0178	0.0784	1.1327	0.0951	1.0777	0.0627
R^2	0.9813	0.9473	0.9730	0.9216	0.9734	0.9571	0.9785	0.9274

TABLE-8
Zn/Fe SELECTIVITY INDEX OF EACH PARTICLE SIZE AND MODEL

S.I.	$d_{80} = 0.180$ mm	$d_{80} = 0.125$ mm	$d_{80} = 0.075$ mm	$d_{80} = 0.063$ mm
Model 1	8.13	15.32	8.87	12.08
Model 2	9.00	18.62	9.93	13.54
Model 3	2.86	8.33	3.38	3.50
Model 4	10.63	25.73	11.91	16.39

CONCLUSIONS

This study has examined the effects of particle size distribution on the flotation behaviour of Turkish sphalerite. Timed batch tests on ground ore using a pilot flotation column and subsequent statistical analysis of experimental data indicated that the optimum feed size for the ore should be $d_{80} = 0.125$ mm. In tests, medium size particles were also observed to form smaller and more stable bubbles, resulting in more efficient flotation. Modelling indicated that a first-order kinetic model incorporating a rectangular distribution of floatabilities gave the best fit for experimental data.

ACKNOWLEDGEMENTS

The authors thank the Cukurova University Scientific Research Projects Directorate for supporting this study (project no. FBE.2002.D.215).

REFERENCES

1. F.B. Castro and M.K. Hoces, *Chem. Engg. Sci.*, **51**, 119 (1996).
2. M. Xu, *Min. Engg.*, **11**, 271 (1998).
3. W.J. Trahar and L.J. Warren, *Int. J. Min. Sci.*, **3**, 103 (1976).
4. G.J. Jameson, *Min. Sci. Engg.*, **9**, 103 (1977).
5. B.P. Radoec, L.B. Alexandrova and S.D. Tchaljovska, *Int. J. Min. Process*, **28**, 127 (1989).
6. G. Morizot, P. Conll, M.V. Durance, Badri, *Int. J. Miner. Process*, **51**, 39 (1997).
7. X.M. Yuan, B.I. Palsson and K.S.E. Forssberg, *Min. Engg.*, **9**, 429 (1996).
8. E.C. Dowling, R.R. Klimpel and F.F. Aplan, *Min. Metallurg. Proc.*, **2**, 87 (1985).
9. A.J. Lynch, N.W. Johnson, E.V. Manlaping and C.G. Thorne, Mineral and coal flotation circuits, Chapter 3: Mathematical models of flotation, in: D.W. Fuerstenau, (advisory editor), *Developments in Mineral Processing*, Elsevier, Amsterdam, pp. 3–57 (1981).
10. M. Xu, P. Quinn and R.S. Crawley, *Min. Engg.*, **9**, 499 (1996).
11. D. Feng and C. Aldrich, *Min. Engg.*, **12**, 721 (1999).

(Received: 11 June 2003; Accepted: 04 December 2003)

AJC-3260

**10th INTERNATIONAL CONFERENCE ON ORGANIC PROCESS
RESEARCH & DEVELOPMENT**

VANCOUVER, CANADA

JULY 13–16, 2004

Contact:

<http://www.scientificupdate.co.uk/>

CHIRAL USA 2004

BOSTON, USA

OCTOBER 4–5, 2004

Contact:

<http://www.scientificupdate.co.uk/>